

Received January 7, 2018, accepted February 1, 2018, date of publication February 12, 2018, date of current version March 15, 2018.

Digital Object Identifier 10.1109/ACCESS.2018.2804903

# Secure Transmission in SWIPT-Powered Two-Way Untrusted Relay Networks

JIAZHEN ZHANG<sup>1,2</sup>, XIAOFENG TAO<sup>1,2</sup>, (Senior Member, IEEE),  
HUICI WU<sup>1</sup>, (Student Member, IEEE), AND XUEFEI ZHANG<sup>1</sup>, (Member, IEEE)

<sup>1</sup>National Engineering Laboratory for Mobile Network Technologies, Beijing University of Posts and Telecommunications, Beijing 100876, China

<sup>2</sup>Beijing University of Posts and Telecommunications Research Institute, Shenzhen, China

Corresponding author: Xiaofeng Tao (taoxf@bupt.edu.cn)

This work was supported in part by the National Key Research and Development Program of China under Grant 2016YFB0800102, in part by the National Natural Science Foundation of China under Grant 61501057 and Grant 61701037, in part by the Shenzhen Science and Technology Innovation Commission Free Exploring Basic Research Project under Project JCYJ20170307172830043, and in part by the 111 Project of China under Grant B16006.

**ABSTRACT** In this paper, we investigate the secure transmission in two-way untrusted amplify-and-forward relay networks with simultaneous wireless information and power transfer (SWIPT). Two secure SWIPT relaying strategies, namely, secure power splitting (SPS) and secure time switching (STS), are studied with the objective of secrecy rate (SR) and secure energy efficiency (SEE) maximization. First, the high signal-to-noise ratio approximations of SR and SEE are established, based on which non-convex SPS-based and convex STS-based SR maximization problems are formulated to jointly optimize the source transmit power and resource division ratio. Suboptimal solutions are obtained by employing Dinkelbach's method and Newton's method, respectively. Furthermore, to guarantee both the energy efficiency and secure quality of service (QoS) performance, SEE maximization problems are formulated with the consideration of the energy harvesting activation constraint and the target SR requirement. The intractable non-convex SEE maximization problems are reformulated as parameter programming, transformed to Lagrange dual problems, and finally solved by two SEE resource allocation algorithms with low complexity. Numerical results verify the convergence and effectiveness of the proposed algorithms and provide new insights into relaying strategy design and secure relay placement.

**INDEX TERMS** Physical layer security, SWIPT, untrusted relay, secure energy efficiency.

## I. INTRODUCTION

Energy-constraint networks such as wireless sensor networks [1], [2] and relay networks [3], consisting of wireless nodes equipped with finite-capacity battery, require periodic battery recharging to maintain continuous network operation. To extend the lifetime of the energy-constraint nodes and exploit external energy source sufficiently, radio frequency (RF)-signal-based simultaneously wireless information and power transfer (SWIPT) was proposed to jointly extract information and replenish energy from the same signal by performing two circuits to separate the information processing and power transfer alternatively [4]. The SWIPT, enabling sustainable operation in a low power area with low expense, provides the advantage of realizing controllable RF energy and information reception [3].

Benefit by the efficient paradigm, the SWIPT technique has been widely applied in energy-constraint relay

networks to support information forwarding and improve energy efficiency [5]. Two relaying strategies, namely the time switching (TS) and the power splitting (PS), were proposed to enable SWIPT at the relay. The receiver switches between two circuits in different phases with TS, and splits the received signal into two portions by power and dedicates them to two circuits simultaneously with PS [6]. The introduction of SWIPT results in weak anti-eavesdropping capability because it is unfavorable for energy-constraint nodes to implement cryptographic technique requiring complex computation resources or sophisticated physical layer security (PLS) schemes requiring extra amount of energy. Besides, the trustworthiness of relay is also a key problem in the SWIPT relay systems since the untrusted relay (UR) performs information forwarding following the transmission strategy but simultaneously may intercept or even interfere the confidential message [7]. As a result, the information

leakage emerges as a considerable problem in the SWIPT relay networks.

So far, conventional PLS techniques such as cooperative jamming [8], [9], secure beamforming [10], [11] and relay placement [12] have been investigated in trusted SWIPT relaying system to guarantee information security. In [8], secrecy rate (SR) was maximized by jointly optimizing the power allocation at transmitter and full-duplex SWIPT jammer in a three-node system. In [9], a harvest-then-jam paradigm of multi-antenna jammers for secure amplify-and-forward (AF) relaying was studied, where the artificial noise covariance matrix and the beamforming matrix were jointly optimized. In [10] and [11], secure relay beamforming problem for SWIPT was investigated in one-way and two-way AF-relay networks separately. In [12], antenna selection schemes and relay selection schemes based on the knowledge of channel state information (CSI) were applied to enhance the security in a TS-based relaying system. In addition to the above fundamental three-node system, secure communication via SWIPT relay was also investigated for Device-to-Device networks [13] and cognitive networks [14] under various setups.

There are also a few existing studies, worked on the design of secure relaying strategy in one-way untrusted SWIPT relay networks. Reference [15] designed optimal transmission strategy at relay with the consideration of destination-based artificial noise to maximize SR. Reference [16] derived analytical expressions for secrecy outage probability and ergodic secrecy rate under both PS and TS policies in a jamming-assisted untrusted one-way relaying system. Reference [17] investigated upper-bound on secrecy outage probability for jamming-assisted untrusted relaying with Alien eavesdropping. Since the realizing of SR maximization is restricted by the energy-constraint feature of RF-powered nodes, [18], [19] selected secure energy efficiency (SEE) as a criteria to evaluate secure communication from a confidential and sustainable perspective.

To the authors' best knowledge, the security issues in two-way untrusted SWIPT relay systems are critical problems yet to be studied. Conventional studies on two-way relay generally considered grid power or battery as energy supply [20]–[22]. We employ SWIPT at UR to provide incentives for relay cooperation since the relay may not be willing to drain limited battery energy to assist transmission. With the introduction of SWIPT, the configuration of time and power division at UR determines the quality of received signals at information receiver and eavesdropper (i.e. UR), which further has a detrimental effect on secrecy performance. Besides, most existing literatures [8]–[17], [23], [24] pursued SR maximization, while the huge energy consumption along with the realizing of superior SR performance poses a threat to the lifetime of SWIPT relay networks. Differently from these prior works, we aim to investigate the tradeoff between the SR and SEE, and approach SEE maximization while guaranteeing secure quality of service (QoS) at a certain level.

Motivated by the above observations, in this paper, we concern with the design of secure relaying strategies in a two-way untrusted SWIPT relay network. To protect confidential messages against UR, the access point (AP) and user equipment (UE) transmit jamming signal and information signal to UR simultaneously. In the downlink direction, the UR replenishes energy from the jamming signal for signal amplification and forwards RF energy to UE for charging. In reverse direction, the UR forwards the confidential information to AP following the predesigned secure transmission strategies. One practical scenario is the sensor networks, where an energy-constraint sensor aims to send information to AP with the help of an idle UE belonging to another network. In a nutshell, the contributions of our paper are three-fold:

1) *Relaying Strategies for Secure Communication*: Two secure SWIPT relaying strategies, namely secure power splitting (SPS) and secure time switching (STS), are performed with the source-assisted jamming. With high signal-to-noise ratio (SNR) regime, the approximated expressions for SR and SEE are developed.

2) *SR and SEE Maximization*: With the objective of SR maximization, we formulate source power allocation and resource division ratio optimization problems for the SPS and STS strategies, which are proved to be non-convex problem and convex problem and are solved by Dinkelbach's method [25] and Newton's method respectively. In order to extend the network lifetime and meanwhile highlight the secure QoS requirement, SEE maximizations with both strategies are formulated subject to the energy harvesting (EH) activation constraint and target SR requirement. To deal with the non-convexity of SEE maximization problems, we reformulate primal problems as parameter programming, transform them into Lagrange dual problems and propose two SEE resource allocation (SRA) algorithms with low complexity.

3) *Numerical Results and Design Insights*: The convergence and effectiveness of the proposed algorithms are verified by comparing with a benchmark method. Numerical results reveal a trade-off between the SR and SEE. With SPS strategy, the SEE achieves a 115.6% improvement with only 12.1% loss in SR, which is significant for secure SWIPT relaying design. When achieving the optimal SEE performance, the SPS-based relay outperforms the STS-based relay with approximate 78.1% gain on SEE and 59.7% gain on SR. Furthermore, we observe that the UR placed close to source under SPS strategy and close to either two ends of source-destination link under STS strategy can provide better secure performance, which is distinct from one-way untrusted relay scenario and two-way trusted relay scenario with the optimal relay position close to the destination [16], [26].

The remainder of this paper is organized as follows. In Section II, the system model as well as the performance metrics of the proposed STS and SPS strategies are presented. In Section III and IV, the mathematical problems of SR and SEE optimization are formulated respectively. We jointly optimize the system parameters utilizing the

proposed solution. The simulation results are shown in Section V. Finally, this paper is summarized in Section VI.

## II. SYSTEM MODEL AND PERFORMANCE METRICS

We consider a two-way untrusted SWIPT relay network, where the destination (UE) intends to send confidential messages to the source (AP) with the assistance of an AF UR (a potential eavesdropper). The AP is powered by on-grid power, while both the UR and UE are energy-constraint nodes equipped with a finite-capacity battery. All the nodes operate in half-duplex mode and there is no direct link between the AP and UE due to severe blockage [6].

The RF signals experience flat block Rayleigh fading and thus the channel coefficients remain unchanged within each transmission slot and vary across slots [27]. Denote  $h_1, h_2$  as the channel coefficients of the AP-UR link and UR-UE link, respectively. Downlink and uplink channel reciprocity are assumed [4] and the channel power gain  $|h_i|^2$  follows exponential distribution with mean  $\rho_i$ :

$$f_{|h_i|^2}(x) = \frac{1}{\rho_i} \exp\left(-\frac{x}{\rho_i}\right), \quad (1)$$

where  $\rho_i = d_i^{-L}$ ,  $d_1$  and  $d_2$  indicate the distance of AP-UR link and UR-UE link, respectively,  $L$  is the path loss exponent.

Both the AP and UE are equipped with a single omnidirectional antenna. The UR owns two single-beam directional antennas which can either be switched to a specific direction arbitrarily or operate in omnidirectional mode [28]. The directional antennas provide the ability to deal with received signals at different antennas separately and have the potential to enhance SEE. We simplify the analysis by modeling the directional antennas with Flattop radiation pattern [29] where the directivity gain within the main beam with beamwidth  $\Theta$  is a constant  $M = \frac{2\pi}{\Theta}$  and the gain outside the beamwidth is ignored.

The total power consumption at AP can be expressed as a linear form [30]:

$$P_T = \alpha P_t + P_a \quad (2)$$

where  $\alpha$  is the power coefficient,  $P_t$  and  $P_a$  account for transmit power and the static power at AP. The harvested energy at UR and UE is assumed to be entirely transformed to radiation power with circuitry power consumption ignored [4]. Moreover, perfect channel state information (CSI) is available at all nodes.<sup>1</sup> In the following, we explain the SPS and STS strategy in detail.

### A. POWER SPLITTING STRATEGY BASED SECURE RELAYING

As shown in Fig. 1, the transmission slot (of duration  $T$ ) is equally divided into two phases. In the first phase, UE transmits the information signal to UR, meanwhile the AP sends a

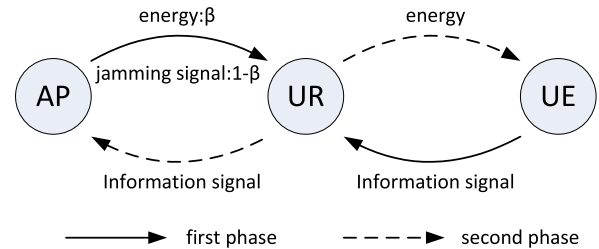


FIGURE 1. Secure power splitting relaying strategy.

jamming signal to UR to charge the relay and maintain information security. The main beams of two directional antennas at UR steer to AP and UE to receive jamming and information signals separately. Denote  $\beta$  as the power division ratio (PDR) for EH with  $0 < \beta \leq 1$ . The amount of energy replenished by UR is

$$E_r = \beta \eta M P_t |h_1|^2 \frac{T}{2}, \quad (3)$$

where  $\eta$  is the EH conversion efficiency factor with  $0 < \eta \leq 1$ , noise power is neglected as compared to transmit power  $P_t$ . The remaining portion of the jamming signal and information signal are combined in information processing circuit [31], which is expressed as

$$y_r = \sqrt{1 - \beta}(\sqrt{M P_t} h_1 x_a + n_0) + \sqrt{M P_u} h_2 x_u + n_1, \quad (4)$$

where  $x_a$  is the unit power jamming signal sent by AP,  $x_u$  is the unit power confidential message sent by UE,  $P_u$  is the transmit power at UE,  $n_0 \sim \mathcal{CN}(0, \sigma_0^2)$  and  $n_1 \sim \mathcal{CN}(0, \sigma_1^2)$  indicate the additive Gaussian noise at two directional antennas with variance  $\sigma_0^2$  and  $\sigma_1^2$  respectively. Thus, the signal-to-interference-plus-noise ratio (SINR) at UR can be written as

$$\Xi_r = \frac{M P_u |h_2|^2}{(1 - \beta) M P_t |h_1|^2 + (1 - \beta) \sigma_0^2 + \sigma_1^2}. \quad (5)$$

In the second phase, UR transmits the amplified signal  $x_r$ , as given in (6), with one omnidirectional antenna.

$$x_r = \sqrt{\kappa} \left( \sqrt{1 - \beta} \sqrt{M P_t} h_1 x_a + \sqrt{M P_u} h_2 x_u + n_r \right), \quad (6)$$

where  $\kappa$  is the amplification coefficient,  $n_r \sim \mathcal{CN}(0, \sigma_r^2)$  is the processing noise at UR. Herein, the additive noise is dominated by  $n_r$  [31] and is ignored for simplicity. Since UR exhausts the harvested energy for transmission (i.e.,  $E_r = E[|x_r|^2] \frac{T}{2}$ ), the amplification coefficient  $\kappa$  can be derived as

$$\kappa = \frac{\beta \eta M P_t |h_1|^2}{(1 - \beta) M P_t |h_1|^2 + M P_u |h_2|^2 + \sigma_r^2}. \quad (7)$$

The received signal at the AP is  $y_a = x_r h_1 + n_2$ , where  $n_2 \sim \mathcal{CN}(0, \sigma_2^2)$  accounts for the additive noise at the AP. The UE always exhausts its available energy for transmission (i.e.  $\eta E[|x_r|^2] |h_2|^2 \frac{T}{2} = P_u \frac{T}{2}$ ), which yields

$$P_u = \beta \eta^2 M P_t |h_1|^2 |h_2|^2. \quad (8)$$

<sup>1</sup>Since the source, relay and destination belong to the same system, perfect CSI at three nodes is considered.

Since the jamming signal  $x_a$  is known to the AP, it can be removed from  $y_a$  through interference cancellation [4]. Combining (6), the received SINR at the AP is given by

$$\Xi_a = \frac{\beta^2 \eta^3 M^3 P_t^2 |h_1|^6 |h_2|^4}{\beta \eta M P_t |h_1|^4 \sigma_r^2 + (M P_t |h_1|^2 \psi + \sigma_r^2) \sigma_2^2}. \quad (9)$$

where  $\psi = 1 - \beta + \beta \eta^2 M |h_2|^4$ . As a result, the instantaneous SR as a function of  $\beta, P_t$  is

$$R_{s,P}(\beta, P_t) = \left[ \frac{1}{2} \log_2 \left( \frac{1 + \Xi_a}{1 + \Xi_r} \right) \right]^+, \quad (10)$$

where  $[x]^+ \triangleq \max\{0, x\}$ . Specifically, in high SNR scenario (i.e.,  $\frac{P_t |h_1|^2}{\sigma_0^2} \gg 1, \frac{P_t |h_1|^2}{\sigma_1^2} \gg 1$ ), we have following approximations:

$$\Xi_r \stackrel{\text{high SNR}}{\approx} \frac{\beta \eta^2 M |h_2|^4}{1 - \beta}, \quad (11)$$

$$1 + \Xi_a \stackrel{\text{high SNR}}{\approx} \Xi_a \stackrel{\sigma_r^2 \sigma_2^2 \ll \sigma_r^2}{\approx} \frac{\beta^2 \eta^3 M^2 P_t |h_1|^4 |h_2|^4}{\beta \eta |h_1|^2 \sigma_r^2 + \psi \sigma_2^2}. \quad (12)$$

The achievable SR is definitely non-negative through system parameter optimization, hence the SR is simplified as

$$R_{s,P}(\beta, P_t) \approx \frac{1}{2} \log_2 \left( \frac{(1 - \beta) \beta^2 \eta^3 M^2 P_t |h_1|^4 |h_2|^4}{\beta \eta |h_1|^2 \sigma_r^2 \psi + \sigma_2^2 \psi^2} \right). \quad (13)$$

The total power consumption of the system within each transmission slot is  $P_{T,P}(P_t) = \frac{1}{2} \alpha P_t + P_a$ . It is worth noting that the available power at both UR and UE is originated from the AP, which is not incorporated in the total power consumption due to its sustainability.

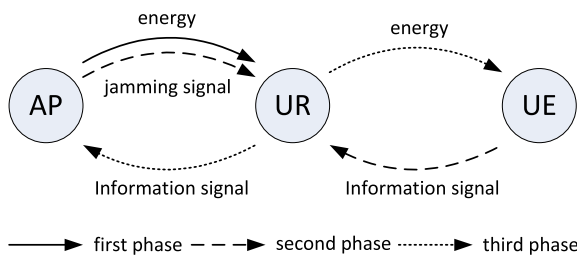


FIGURE 2. Secure time switching relaying strategy.

### B. TIME SWITCHING STRATEGY BASED SECURE RELAYING

A secure time-switching relaying strategy is shown in Fig. 2, where two antennas at UR work in directional mode when receiving while one antenna works in omnidirectional mode when transmitting. Denote  $\tau$  as time division ratio (TDR) for EH with  $0 < \tau \leq 1$ . The first phase of duration  $\tau T$  is dedicated to transmitting jamming signal to UR for charging, during which the amount of harvested energy is  $E_r = \eta M P_t |h_1|^2 \tau T$ . In the second phase of duration  $(1 - \tau) \frac{T}{2}$ , the received signal at UR is  $y_r = \sqrt{M P_t} h_1 x_a + \sqrt{M P_u} h_2 x_u + n_0 + n_1$ . It should be declared that the signal transmission

at UE is initialized with remaining battery energy before EH process<sup>2</sup> [26], [32]. In the third phase, UR forwards amplified signal  $x_r = \sqrt{\kappa} (\sqrt{M P_t} h_1 x_a + \sqrt{M P_u} h_2 x_u + n_r)$  to AP and the same signal to UE for charging.

Recall that the signal radiation drains the harvested energy at UR and UE, i.e.,  $E_r = E[|x_r|^2] \frac{(1 - \tau) T}{2}, \eta E[|x_r|^2] |h_2|^2 = P_u$ .  $\kappa$  and  $P_u$  are derived as

$$\kappa = \frac{2 \eta \tau M P_t |h_1|^2}{(1 - \tau) (M P_t |h_1|^2 + M P_u |h_2|^2 + \sigma_r^2)}, \quad (14)$$

$$P_u = \frac{2 \eta^2 \tau M P_t |h_1|^2 |h_2|^2}{1 - \tau}. \quad (15)$$

The received SINR at AP and UR is  $\Xi_a = \frac{\kappa M P_u |h_1|^2 |h_2|^2}{\kappa |h_1|^2 \sigma_r^2 + \sigma_2^2}$  and  $\Xi_r = \frac{M P_u |h_2|^2}{M P_t |h_1|^2 + \sigma_0^2 + \sigma_1^2}$  respectively. With high SNR regime, we have approximations  $1 + \Xi_r \approx \frac{1 - \tau + 2 \eta^2 |h_2|^4 \tau M}{1 - \tau}$  and  $1 + \Xi_a \approx \Xi_a$ , and SR is given by

$$R_{s,T}(\tau, P_t) \approx \frac{1 - \tau}{2} \log_2 \left( \frac{4 |h_1|^4 |h_2|^4 \tau^2 \eta^3 M^2 P_t}{2 \eta \tau |h_1|^2 \sigma_r^2 \psi + \sigma_2^2 \psi^2} \right). \quad (16)$$

where  $\psi = 1 - \tau + 2 \eta^2 M |h_2|^4 \tau$ . Within each transmission slot, the total power consumption of such a system is  $P_{T,T}(\tau, P_t) = \frac{1 + \tau}{2} \alpha P_t + P_a$ .

## III. FORMULATION AND ANALYSIS OF SECRECY RATE MAXIMIZATION PROBLEM

In this section, the transmit power at AP and resource division ratio at UR are jointly optimized with the objective of SR maximization under both relaying strategies. The suboptimal solutions are obtained iteratively by employing Dinkelbach's method and Newton's method respectively.

### A. SPS STRATEGY

#### 1) PROBLEM FORMULATION

To determine the optimal SPS strategy, the SR maximization problem can be formulated as follows:

$$\max_{\{\beta, P_t\}} \frac{1}{2} \log_2 \left( \frac{a(1 - \beta) \beta^2 P_t}{b \beta (1 - \beta + c \beta) + d (1 - \beta + c \beta)^2} \right) \quad (P1)$$

$$s.t. \quad 0 < \beta \leq 1 \quad (17a)$$

$$0 < P_t \leq P_{max} \quad (17b)$$

$$g P_t \geq \theta \quad (17c)$$

$$h \beta P_t \geq \theta \quad (17d)$$

where  $a \triangleq M^2 |h_1|^4 |h_2|^4 \eta^3, b \triangleq |h_1|^2 \eta \sigma_r^2, c \triangleq \eta^2 M |h_2|^4, d \triangleq \sigma_2^2, g \triangleq M |h_1|^2, h \triangleq \eta M |h_1|^2 |h_2|^2, \theta$  is the activation threshold of EH circuit,  $P_{max}$  is the peak transmit power at AP. (17c) and (17d) follow from  $P_t |h_1|^2 M \geq \theta$  and  $E[|x_r|^2] |h_2|^2 \geq \theta$  respectively, which specify the constraints

<sup>2</sup>When the UE is activated for the first time, the transmit power at UE originates from the initial battery energy. Afterwards, since the UR and UE follow the energy-causality constraint that the energy consumption does not exceed the amount of harvested energy during former phase, the relay system is assured to operate in an sustainable manner.



on EH activation power at UR and UE. The EH circuit activation constraint is absorbed therein to support higher power sensitivities at typical EH receivers comparing with general information receivers [2].

2) ANALYSIS AND SUBOPTIMAL SOLUTION

In this subsection, we firstly discuss the monotonicity of the objective function of (P1) with respect to (w.r.t.)  $P_t$ . Since SR monotonically increases with  $P_t$  over feasible region  $P_t \in (\min\{\frac{\theta}{g}, \frac{\theta}{h\beta}\}, P_{max})$ , the optimal SR is achieved with  $P_t = P_{max}$ . The non-convexity of SR w.r.t.  $\beta$  makes it challenging to optimize  $\beta$  theoretically. Calculating the optimal  $\beta$  through one-dimension exhaustive searching incurs great computational complexity. To reduce the computational complexity, we transform the primal problem (P1) into a subtractive form by introducing parameter  $\lambda$  [25]:

$$\begin{aligned} & \max_{\{\beta\}} (1-\beta)\beta^2 - \lambda [b\beta(1-\beta+c\beta) + d(1-\beta+c\beta)^2] \\ & \text{s.t. } \frac{\theta}{hP_{max}} < \beta \leq 1 \end{aligned} \quad \times(\mathbf{P1}^{(1)}) \quad (18)$$

Define  $D(\lambda) = (1-\beta)\beta^2 - \lambda [b\beta(1-\beta+c\beta) + d(1-\beta+c\beta)^2]$ ,  $F(\beta) = D(\lambda)$ . Denote  $\beta^*$  as the feasible PDR at UR. The suboptimal SR  $\lambda^*$  can be achieved only when  $\lambda^*$  and  $\beta^*$  satisfy

$$\begin{aligned} & \max_{\{\beta\}} (1-\beta)\beta^2 - \lambda^* [b\beta(1-\beta+c\beta) + d(1-\beta+c\beta)^2] \\ & = (1-\beta^*)\beta^{*2} - \lambda^* \\ & \times [b\beta^*(1-\beta^*+c\beta^*) + d(1-\beta^*+c\beta^*)^2] = 0. \end{aligned} \quad (19)$$

Dealing with (P1<sup>(1)</sup>) is equivalent to determining  $\lambda^*$  that satisfying  $D(\lambda^*) = 0$ , as described in Algorithm 1. In each iteration, suboptimal  $\beta$  is obtained with a given  $\lambda$  by applying Theorem 1. The  $\lambda$  in next iteration is updated by  $\lambda = \frac{(1-\beta)\beta^2}{b\beta(1-\beta+c\beta)+d(1-\beta+c\beta)^2}$ . Algorithm 1 continues until  $D(\lambda)$  is below the predetermined gap  $\epsilon$ , i.e.,  $|D(\lambda)| < \epsilon$ .

**Algorithm 1** Iterative SR (SEE) Optimization Based on Dinkelbach’s Method

**Input:**  $\lambda$   
**Output:**  $\lambda, \beta^*(\beta^* \text{ or } \tau^*), P_t^*$   
 1: **do**  
 2:  $P_t^* = P_{max}$ , Determine  $\beta^*$  by applying Theorem 1 (or Determine  $P_t^*, \beta^* \text{ or } \tau^*$  by applying Algorithm 2);  
 3:  $\lambda \leftarrow \frac{(1-\beta)\beta^2}{b\beta(1-\beta+c\beta)+d(1-\beta+c\beta)^2}$  (or  $\lambda \leftarrow \frac{R_s(\beta^* \text{ or } \tau^*, P_t^*)}{P_t(P_t^*)}$ )  
 4: **while** ( $|D(\lambda)| > \epsilon$ )

*Theorem 1:* For the maximization of SR under SPS strategy, the suboptimal PDR of problem (P1<sup>(1)</sup>) is

given by

$$\beta^* = \begin{cases} \arg \max_{\beta \in \{\frac{\theta}{hP_{max}}, r_2\}} F(\beta) & \frac{\theta}{hP_{max}} \leq r_2 \leq 1 \\ \frac{\theta}{hP_{max}} & r_2 < \frac{\theta}{hP_{max}} \\ \arg \max_{\beta \in \{\frac{\theta}{hP_{max}}, 1\}} F(\beta) & 1 < r_2, \end{cases} \quad (20)$$

where  $r_i = \frac{G(\lambda) \pm \sqrt{G(\lambda)^2 - 6d\lambda(c-1) - 3b\lambda}}{3}$  with  $i \in \{1, 2\}$  and  $r_1 < r_2$ ,  $G(\lambda) = 1 - b\lambda(c-1) - d\lambda(c-1)^2$ .

*Proof:* Taking the derivatives of  $F(\beta)$  w.r.t.  $\beta$ , we have

$$\begin{aligned} \frac{\partial F(\beta)}{\partial \beta} &= -3\beta^2 + 2\beta - 2b\lambda(c-1)\beta \\ &\quad - 2d\lambda(c-1)^2\beta - [2d(c-1) + b]\lambda = 0. \end{aligned} \quad (21)$$

Denote by  $r_1, r_2$  the two real roots of quadratic equation (21). Consequently,  $F(\beta)$  decreases with  $\beta$  when  $\beta < r_1$  or  $\beta > r_2$ , whereas increases with  $\beta$  when  $r_1 \leq \beta \leq r_2$ . Taking the feasible region of  $\beta$  into account, we determine suboptimal  $\beta$  via case studies: a) if the local optimal point  $\beta = r_2$  locates in feasible region, the feasible solution is selected between local optimal point and lower bound of feasible region, i.e.  $\arg\max\{F(\frac{\theta}{hP_{max}}), F(r_2)\}$ ; b) if  $r_2 < \frac{\theta}{hP_{max}}$ , the maximum  $F(\beta)$  is achieved at lower bound of feasible region; c) if  $r_2 > 1$ ,  $F(\beta)$  is maximized at upper or lower bound of feasible region. ■

**B. STS STRATEGY**

1) PROBLEM FORMULATION

To determine the optimal STS strategy, we formulate the SR optimization problem as follow:

$$\max_{\{\tau, P_t\}} \frac{1-\tau}{2} \log_2 \left( \frac{aP_t\tau^2}{b\tau(1-\tau+c\tau)+d(1-\tau+c\tau)^2} \right) \quad (\mathbf{P2})$$

$$\text{s.t. } 0 < \tau \leq 1 \quad (22a)$$

$$0 < P_t \leq P_{max} \quad (22b)$$

$$P_t g \geq \theta \quad (22c)$$

$$\theta\tau + h\tau P_t \geq \theta \quad (22d)$$

where  $a \triangleq 4|h_1|^4|h_2|^4\eta^3M^2$ ,  $b \triangleq 2\eta|h_1|^2\sigma_r^2$ ,  $c \triangleq 2\eta^2M|h_2|^4$ ,  $d \triangleq \sigma_s^2$ ,  $g \triangleq |h_1|^2M$ ,  $h \triangleq 2\eta M|h_1|^2|h_2|^2$ , (22c) and (22d) ensure the EH activation condition at UR and UE.

2) EXISTENCE AND UNIQUENESS OF THE OPTIMAL SOLUTION TO (P2)

*Proposition 1:* (P2) is a convex optimization problem w.r.t.  $\tau$  and  $P_t$ . The global optimum of (P2) exists and is unique.

*Proof:* (P2) is a convex problem w.r.t.  $\tau$  and  $P_t$  due to the non-negative definitivity of Hessian matrix of the objective function and the convexity of the constraint functions (22a)-(22d), which can be verified numerically and is omitted here. ■

3) ANALYSIS AND OPTIMAL SOLUTION

The optimal solution to STS-based SR maximization is given by the following theorem.

**Theorem 2:** For the maximization of SR under STS strategy, we select peak transmit power at AP and obtain the optimal TDR by applying Newton’s method over  $\tau \in \left(\frac{\theta}{\theta+hP_{max}}, 1\right)$ .

*Proof:* Similarly as in Theorem 1, AP always transmits at maximum power due to the monotonically increasing of SR w.r.t.  $P_t$ . Define  $F(\tau) = \frac{1-\tau}{2} \log_2 \left( \frac{a\tau^2}{b\tau(1-\tau+c\tau)+d(1-\tau+c\tau)^2} \right)$ . The first-order derivative  $\frac{\partial F(\tau)}{\partial \tau}$  is positive with  $\tau \rightarrow 0$  and negative with  $\tau \rightarrow 1$ . Therefore, there exists a unique solution satisfying  $\frac{\partial F(\tau)}{\partial \tau} = 0$ , which is intractable considering the involved logarithmic form. Alternatively, we obtain the optimal TDR via one-dimensional searching over a shrinking feasible region. ■

**IV. FORMULATION AND ANALYSIS OF SECURE ENERGY EFFICIENCY MAXIMIZATION PROBLEM**

In this section, to improve network energy efficiency with the guarantee of secure QoS requirement, we maximize the SEE subject to the EH activation power constraint and minimum SR requirement. To deal with the intractable non-convex SEE optimization problems, we reformulate, decompose primal problems into sub-problems and propose SRA algorithms to obtain suboptimal solution with low complexity.

**A. SPS STRATEGY**

**1) PROBLEM FORMULATION**

Recall that SEE is defined as the ratio of SR to total power consumption. The SEE optimization problem is formulated as follow:

$$\max_{\{\beta, P_t\}} \frac{\log_2 \left( \frac{a(1-\beta)\beta^2 P_t}{b\beta(1-\beta+c\beta)+d(1-\beta+c\beta)^2} \right)}{eP_t + f} \tag{P3}$$

s.t. (17a)-(17d)

$$R_{s,P}(\beta, P_t) \geq R_{th} \tag{23}$$

where  $e \triangleq \alpha$ ,  $f \triangleq 2P_a$ , (23) ensures the reliability of transmission and this system will suffer from information leakage if (23) is violated. Note that notations a~d, g, h in this subsection is the same as that in Section III. A. Taking all constraints into account, the feasible region  $\mathcal{R}_P$  of (P3) is

$$\mathcal{R}_P = \{(\beta, P_t) | 0 < \beta \leq 1, P_{min,P}(\beta) \leq P_t \leq P_{max}\}, \tag{24}$$

where

$$P_{min,P}(\beta) \triangleq \max \left\{ 2^{2R_{th}} \frac{b\beta(1-\beta+c\beta)+d(1-\beta+c\beta)^2}{a(1-\beta)\beta^2}, \frac{\theta}{g}, \frac{\theta}{h\beta} \right\}.$$

**2) EQUIVALENT PROBLEM FORMULATION**

(P3) is non-convex due to the fractional form of objective function. Similarly as in Section III. A, we transform the fractional optimization problem (P3) as follow:

$$\max_{\{\beta, P_t\} \in \mathcal{R}_P} R_{s,P}(\beta, P_t) - \lambda P_{T,P}(P_t), \tag{P3^{(1)}}$$

which is equivalent to

$$\min_{\{\beta, P_t\} \in \mathcal{R}_P} \lambda P_{T,P}(P_t) - R_{s,P}(\beta, P_t). \tag{P3^{(2)}}$$

**3) ALGORITHM IMPLEMENTATION**

Define  $D(\lambda) = \lambda P_{T,P}(P_t) - R_{s,P}(\beta, P_t)$ . Denote by  $P_t^*$  the feasible transmit power at AP. The suboptimal SEE  $\lambda^*$  can be achieved only when  $\lambda^*, \beta^*, P_t^*$  satisfy

$$\begin{aligned} \max_{\{\beta, P_t\} \in \mathcal{R}_P} \{ & R_{s,P}(\beta, P_t) - \lambda^* P_{T,P}(P_t) \} \\ & = R_{s,P}(\beta^*, P_t^*) - \lambda^* P_{T,P}(P_t^*) = 0. \end{aligned} \tag{25}$$

The Dinkelbach’s method in Algorithm 1 can be applied to determining  $\lambda^*$  that satisfying  $D(\lambda^*) = 0$ . In each iteration, feasible set  $\{\beta, P_t\}$  are obtained with a given  $\lambda$  by applying Algorithm 2 (i.e. SRA algorithm). The  $\lambda$  in next iteration is updated by  $\lambda = \frac{R_{s,P}(\beta, P_t)}{P_{T,P}(P_t)}$ . Algorithm 1 continues until  $D(\lambda)$  is below the predetermined gap  $\varepsilon$ .

**Algorithm 2** SEE Resource Allocation Algorithm for SPS (STS) Strategy

**Input:**  $(\lambda, \mu [0], \nu [0], \omega [0]), q [0] \leftarrow 0, n \leftarrow 0$

**Output:**  $\beta^*(or \tau^*), P_t^*$

- 1: **do**
- 2:  $n \leftarrow n + 1$ ;
- 3: Determine  $\beta^*(or \tau^*)$  by one-dimensional searching;
- 4: Determine  $P_t^*$  by applying Theorem 3 (or Theorem 4);
- 5: Update  $\mu [n]$  by using (34) (or (44));
- 6: Update  $\nu [n]$  by using (35) (or (45));
- 7: Update  $\omega [n]$  by using (36);
- 8:  $q [n] \leftarrow Q(\lambda, \mu [n], \nu [n], \omega [n])$ ;
- 9: **while**  $(|q [n] - q [n - 1]| > \varepsilon)$

Afterwards, for a given  $\lambda$ , we apply Lagrange dual approach [33] to obtain the suboptimal solution to (P3<sup>(2)</sup>). (P3<sup>(2)</sup>) is still a non-convex optimization problem considering the non-convexity of  $R_{s,P}(\beta, P_t)$ , and the duality gap may exist when solving the dual problem. Separating the variables in (17c)(17d)(23) and incorporating (17c)(17d)(23), the lagrangian of problem (P3<sup>(2)</sup>) is expressed as

$$\begin{aligned} L(P_t, \beta, \lambda, \mu, \nu) &= \lambda(eP_t + f) \\ &\quad - \log_2 \left( \frac{a(1-\beta)\beta^2 P_t}{b\beta(1-\beta+c\beta)+d(1-\beta+c\beta)^2} \right) \\ &\quad + \mu(\theta - gP_t) + \nu(-hP_t + \frac{\theta}{\beta}) \\ &\quad + \omega \left( -P_t + 2^{2R_{th}} \frac{b\beta(1-\beta+c\beta)+d(1-\beta+c\beta)^2}{a(1-\beta)\beta^2} \right) \\ &= \lambda f + \mu\theta + \varphi_1(P_t, \lambda, \mu, \nu, \omega) + \varphi_2(\beta, \nu, \omega) \end{aligned} \tag{26}$$

where  $\mu, \nu, \omega$  are non-negative Lagrange multipliers corresponding to (17c), (17d), (23) respectively, the constraints (17a), (17b) are not absorbed in lagrangian and will be

checked later, and

$$\begin{aligned} \varphi_1(P_t, \lambda, \mu, \nu, \omega) &= \lambda e P_t - \log_2 P_t - \mu g P_t - \nu h P_t - \omega P_t, \end{aligned} \quad (27)$$

$$\begin{aligned} \varphi_2(\beta, \nu, \omega) &= -\log_2 \left( \frac{a(1-\beta)\beta^2}{b\beta(1-\beta+c\beta)+d(1-\beta+c\beta)^2} \right) \\ &+ \frac{\nu\theta}{\beta} + \omega \frac{b\beta(1-\beta+c\beta)+d(1-\beta+c\beta)^2}{a(1-\beta)\beta^2} 2^{2R_{th}}. \end{aligned} \quad (28)$$

The dual problem of **(P3)**<sup>(2)</sup> is

$$\max_{\lambda \geq 0, \mu \geq 0, \nu \geq 0, \omega \geq 0} Q(\lambda, \mu, \nu, \omega), \quad (29)$$

where the dual function is

$$Q(\lambda, \mu, \nu, \omega) = \inf_{\{\beta, P_t\} \in \mathcal{R}_P} L(P_t, \beta, \lambda, \mu, \nu, \omega). \quad (30)$$

Since the variables  $\beta, P_t$  are not coupled in (30), we can decompose the dual function into two sub-problems as follow:

$$\begin{aligned} \inf_{\{\beta, P_t\} \in \mathcal{R}_P} L(P_t, \beta, \lambda, \mu, \nu, \omega) &= \lambda f + \mu \theta + \inf_{\{P_t\} \in \mathcal{P}} \varphi_1(P_t, \lambda, \mu, \nu, \omega) + \inf_{\{\beta\} \in \mathcal{B}} \varphi_2(\beta, \nu, \omega), \end{aligned} \quad (31)$$

where  $\mathcal{B}$  and  $\mathcal{P}$  are the feasible region of  $\beta$  and  $P_t$  while other variables are known. We minimize the  $\varphi_1$  and  $\varphi_2$  term by adjusting AP transmit power and PDR respectively. Notice that (17d)(23) should be met by both parts while solving two sub-problems.

**Theorem 3:** For a given  $\beta$ , the suboptimal AP transmit power of the dual problem is given by

$$P_t^* = \begin{cases} P_{\min, P}(\beta) & P_t' < P_{\min, P}(\beta) \\ P_t' & P_{\min, P}(\beta) \leq P_t' \leq P_{\max} \\ P_{\max} & P_{\max} < P_t', \end{cases} \quad (32)$$

where  $P_t' = \frac{1}{(\lambda e - \mu g - \nu h - \omega) \ln 2}$ .

*Proof:* By differentiating  $\varphi_1$  term w.r.t.  $P_t$ , we have

$$\frac{\partial \varphi_1(P_t, \lambda, \mu, \nu, \omega)}{\partial P_t} = \lambda e - \frac{1}{P_t \ln 2} - \mu g - \nu h - \omega. \quad (33)$$

Since  $\frac{\partial \varphi_1(P_t, \lambda, \mu, \nu, \omega)}{\partial P_t}$  is a monotonically increasing function of  $P_t$ , there exists unique  $P_t' = \frac{1}{(\lambda e - \mu g - \nu h - \omega) \ln 2}$  that satisfying  $\frac{\partial \varphi_1(P_t, \lambda, \mu, \nu, \omega)}{\partial P_t} = 0$ . Consequently, the  $\varphi_1$  term decreases with  $P_t$  when  $P_t < P_t'$ , whereas increases with  $P_t$  when  $P_t > P_t'$ . We determine the suboptimal value of  $P_t$  via case studies: a) if  $P_t' < P_{\min, P}(\beta)$ , the  $\varphi_1$  term increases with  $P_t$  over the feasible region, thus we obtain minimum  $\varphi_1$  with  $P_t^* = P_{\min, P}(\beta)$ ; b) if  $P_{\min, P}(\beta) \leq P_t' \leq P_{\max}$ , the suboptimal solution is achieved at global minimum point, i.e.,  $P_t^* = P_t'$ ; c) if  $P_{\max} < P_t'$ , the  $\varphi_1$  term decreases with  $P_t$ , i.e.  $P_t^* = P_{\max}$ . ■

We next derive the suboptimal PDR at UR by solving  $\inf_{\{\beta\} \in \mathcal{B}} \varphi_2(\beta, \nu, \omega)$ . It can be verified that  $\varphi_2(\beta, \nu, \omega)$  is a continuous but non-convex function of  $\beta$ . The suboptimal PDR can be calculated numerically over the range  $\beta \in \left(\frac{\theta}{hP_t}, 1\right)$ .

Given  $\{\beta, P_t\}$ , Lagrange multipliers  $\mu, \nu, \omega$  are updated by a gradient method as follow:

$$\mu[n+1] = [\mu[n] - \Delta_1(-gP_t + \theta)]^+ \quad (34)$$

$$\nu[n+1] = \left[ \nu[n] - \Delta_2\left(-hP_t + \frac{\theta}{\beta}\right) \right]^+ \quad (35)$$

$$\begin{aligned} \omega[n+1] &= \left[ \omega[n] - \Delta_3(-P_t + 2^{2R_{th}} \right. \\ &\times \left. \frac{b\beta(1-\beta+c\beta)+d(1-\beta+c\beta)^2}{a(1-\beta)\beta^2} \right]^+, \end{aligned} \quad (36)$$

where  $\Delta_1, \Delta_2, \Delta_3$  are sufficiently small step lengths to ensure convergence.

In conclusion, we formalize an optimization algorithm as described in Algorithm 2. Firstly, we initialize the Lagrange multipliers. Next, for a given set of multipliers, we assign transmit power at AP as given in Theorem 3 and conduct the process of PDR configuration. We iterate this process by updating the Lagrange multipliers using the gradient method until the dual function reaches convergence.

Define  $\delta$  the exhaustive search accuracy. The complexity of the optimal exhaustive search is  $\mathcal{O}(\frac{1}{\delta^2})$ , while the complexity for the proposed algorithms is  $\mathcal{O}(\frac{1}{\delta})$ , which comes from the searching of resource division ratio over a shrinking region.

## B. STS STRATEGY

### 1) PROBLEM FORMULATION

Given that STS strategy is applied at UR, the SEE optimization problem is formulated as follow:

$$\begin{aligned} \max_{\{\tau, P_t\}} & \frac{(1-\tau)\log_2\left(\frac{aP_t\tau^2}{b\tau(1-\tau+c\tau)+d(1-\tau+c\tau)^2}\right)}{(1+\tau)eP_t+2f} \quad (\mathbf{P4}) \\ \text{s.t. (23a)-(23d)} & \end{aligned}$$

$$R_{s,T}(\tau, P_t) \geq R_{th} \quad (37)$$

where  $e \triangleq \alpha, f \triangleq P_a$ , the change of variables  $a \sim d, g \sim h$  is the same as that in Section III. B. Denote  $\tau^*$  as the feasible TDR at UR. The feasible region  $\mathcal{R}_T$  of **(P4)** is

$$\mathcal{R}_T = \{(\tau, P_t) \mid 0 < \tau \leq 1, P_{\min, T}(\tau) \leq P_t \leq P_{\max}\}, \quad (38)$$

where  $P_{\min, T}(\tau) \triangleq \max\left\{\frac{(1-\tau+c\tau)b\tau+(1-\tau+c\tau)^2d}{a\tau^2} 2^{\frac{2R_{th}}{1-\tau}}, \frac{\theta}{g}, \frac{\theta-\theta\tau}{h\tau}\right\}$ .

### 2) EQUIVALENT PROBLEM FORMULATION

We formulate an equivalent optimization problem **(P4)**<sup>(1)</sup> with parameter  $\lambda$  as follow:

$$\min_{\{\tau, P_t\} \in \mathcal{R}_T} \lambda P_{T,T}(\tau, P_t) - R_{s,T}(\tau, P_t). \quad (\mathbf{P4}^{(1)})$$

3) EXISTENCE AND UNIQUENESS OF THE OPTIMAL SOLUTION TO  $(\mathbf{P4}^{(1)})$

*Proposition 2:*  $(\mathbf{P4}^{(1)})$  is a convex optimization problem w.r.t.  $\tau$  and  $P_t$ . The global optimum of  $(\mathbf{P4}^{(1)})$  exists and is unique.

*Proof:* The proof of the convexity of  $(\mathbf{P4}^{(1)})$  is omitted here for simplicity. ■

4) ALGORITHM IMPLEMENTATION

The Lagrangian of problem  $(\mathbf{P4}^{(1)})$  is given by

$$L(P_t, \tau, \lambda, \mu, \nu) = \lambda((1 + \tau)eP_t + 2f) - \frac{(1-\tau)(\nu+2)}{2} \log_2 \left( \frac{aP_t\tau^2}{(1-\tau+c\tau)b\tau+(1-\tau+c\tau)^2d} \right) + \mu(\theta - \theta\tau - hP_t\tau) + \nu R_{th}. \quad (39)$$

The dual problem of (40) is

$$\max_{\lambda \geq 0, \mu \geq 0, \nu \geq 0} Q(\lambda, \mu, \nu), \quad (40)$$

where the dual function is

$$Q(\lambda, \mu, \nu) = \inf_{\{\tau, P_t\} \in \mathcal{R}_T} L(P_t, \tau, \lambda, \mu, \nu). \quad (41)$$

Since the variables  $\tau, P_t$  are coupled in (41), we can not decompose the dual function into two portions. Instead, by taking the derivatives of (41) w.r.t.  $\tau$  and  $P_t$ , the following condition can be utilized.

$$\frac{\partial L}{\partial P_t} = \lambda(1 + \tau)e - \frac{(1-\tau)(\nu+2)}{2 \ln 2 P_t} - \mu h \tau = 0 \quad (42)$$

*Theorem 4:* For a given  $\tau$ , the suboptimal AP transmit power of problem  $(\mathbf{P4}^{(1)})$  is given by

$$P_t^* = \begin{cases} P_{min,T}(\tau) & P_t' < P_{min,T}(\tau) \\ P_t' & P_{min,T}(\tau) \leq P_t' \leq P_{max} \\ P_{max} & P_{max} < P_t', \end{cases} \quad (43)$$

where  $P_t' = \frac{(1-\tau)(\nu+2)}{2 \ln 2 (\lambda(1+\tau)e - \mu h \tau)}$ .

*Proof:* Since  $\frac{\partial L}{\partial P_t}$  is a monotonically increasing function of  $P_t$ , there exists unique  $P_t'$  that satisfy  $\frac{\partial L}{\partial P_t} = 0$ . We determine the suboptimal value of  $P_t$  via case studies as the proof of Theorem 3. ■

Due to the intractability of  $\tau^*$ , we search it over the range  $\tau \in \left(\frac{\theta}{\theta+hP_t}, 1\right)$ . Given  $\{\tau, P_t\}$ , Lagrange multipliers  $\mu, \nu$  are updated iteratively as follow:

$$\mu[n+1] = [\mu[n] - \Delta_1(\theta - \theta\tau - hP_t\tau)]^+, \quad (44)$$

$$\nu[n+1] = \left[ \nu[n] - \Delta_2 \left( -\frac{1-\tau}{2} \log_2 \left( \frac{aP_t\tau^2}{(1-\tau+c\tau)(b\tau+(1-\tau+c\tau)d)} \right) + R_{th} \right) \right]^+. \quad (45)$$

V. NUMERICAL RESULTS

In this section, we numerically evaluate the effectiveness of the analytical results and the proposed solutions. Exhaustive search is provided as a benchmark for comparison. The impact of different system parameters on SR and SEE under both strategies is discussed.

A. SYSTEM PARAMETERS AND SIMULATION SETUP

The following system parameters are considered unless stated additionally. The UE is located at the distance  $D = 10$  meters (m) of the AP, and the UR is on the line connecting the AP and UE, i.e.,  $D = d_1 + d_2$ . The far-field SWIPT is considered in this paper, i.e.,  $d_1 > 1\text{m}, d_2 > 1\text{m}$  [4]. Since we optimize secure performance in a slot,  $|h_i|^2$  is set to  $d_i^{-L}$  for simplicity, where path loss exponent  $L$  is 2.7 [16]. We set the EH efficiency, EH circuitry activation threshold, beamwidth of directional antennas to be  $\eta = 0.8, \theta = -10\text{dBm}$  [4],  $\Theta = \frac{\pi}{3}$  respectively. For power consumption model of the AP, the power coefficient and the static power at AP are set as  $\alpha = 8, P_a = 4.8$  watts (W) respectively. The peak power constraint at the AP and target SR are considered  $P_{max} = 2$  watts (W),  $R_{th} = 8$  bps/Hz. The noise variances at all nodes are  $-124\text{dBm}$  [26]. The convergence gap  $\varepsilon$  and exhaustive search accuracy  $\delta$  are at  $10^{-5}$ , which is relatively accurate with acceptable computational complexity.

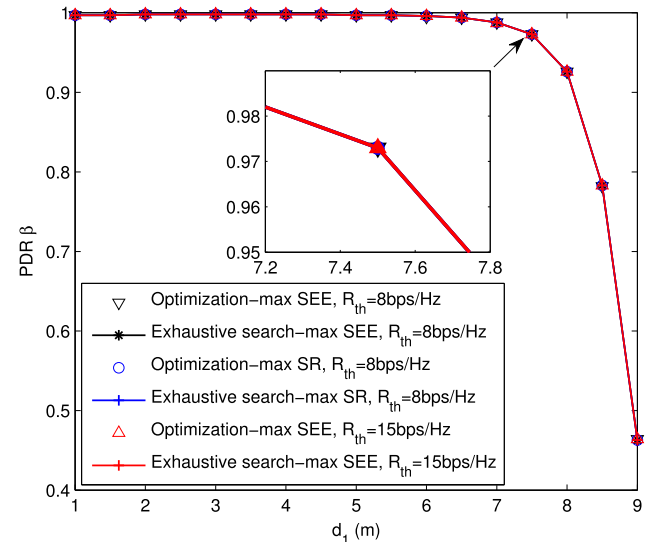


FIGURE 3. PDR for different optimization problems with the implementation of SPS strategy.

B. EFFECT OF RELAY NODE LOCATIONS

Fig. 3 and Fig. 4 demonstrate the PDR  $\beta$  and AP transmit power  $P_t$  for SPS strategy versus  $d_1$ . It is observed that the proposed algorithm can achieve near-optimal solution compared with the results of exhaustive search. For SEE maximization problem with  $d_1 \leq D/2, \beta$  remains quite close to 1 and  $P_t$  increase as UR moves towards UE. In this case, the path loss of AP-UR and UR-UE link determines the amount of harvested energy at UE, and the main problems lie in the EH circuit activation and the



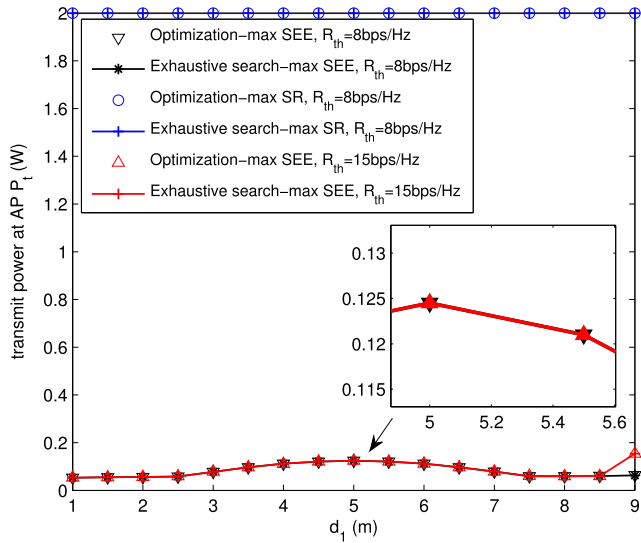


FIGURE 4. AP transmit power for different optimization problems with the implementation of SPS strategy.

maintenance of information processing at UE. With the increasing of  $d_1$ ,  $P_u$  reduces since the superposed effect of path loss of both links become stronger (i.e.  $|h_1|^2 |h_2|^2$  becomes smaller). In the process of uplink transmission, the information signal sent by UE experiences the same path loss as in downlink. That is, the path loss has double effect on  $\Xi_a$  as shown in (9). The SR and SEE, which are dominated by  $\Xi_a$ , decreases with the increasing of  $d_1$ . As a result, when AP transmit power increases to resist path loss and a large portion of harvested energy flows to EH circuit at UR to forward more energy to UE, the information processing at UE is enabled and secure performance is improved.

When UR is close to the UE (i.e.,  $d_1 \geq D/2$ ),  $\beta$  jointly with  $P_t$  decreases as UR moves towards UE. We know from (11) that  $\Xi_r$  is only related to  $\beta$  and  $d_2$ . With the shortening of the distance of UR-UE link, the remaining energy for jamming signal is enhanced to interfere the strengthened information signal at UR. The harvested energy at UE increases with the increasing of  $d_1$  since the superposed effect of path loss becomes weaker (i.e.  $|h_1|^2 |h_2|^2$  becomes larger). Consequently, a comparatively small AP transmit power can contribute to high SEE meanwhile guarantee SR at a certain level.

For SR maximization problem,  $P_t$  remains the maximum value over all  $d_1$ , and  $\beta$  remains the same with that in SEE maximization circumstance. This is due to that once SR target is ensured (i.e. the same feasible region is shared), both SR and SEE performance are maximized when the common item  $\log_2 \left( \frac{a(1-\beta)\beta^2}{b\beta(1-\beta+c\beta)+d(1-\beta+c\beta)^2} \right)$  achieves optimal value. That is, both maximization problems share the same optimal PDR value.

Fig. 5 and Fig. 6 illustrate the TDR and AP transmit power for STS strategy versus  $d_1$ . For SEE maximization problem, the near-optimal  $\tau$  and  $P_t$  first increase and then decrease with  $d_1$ . When UR moves towards UE with

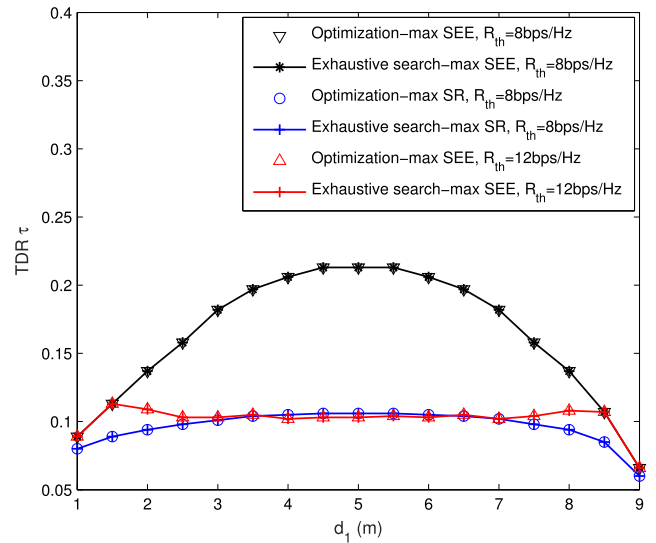


FIGURE 5. TDR for different optimization problems with the implementation of STS strategy.

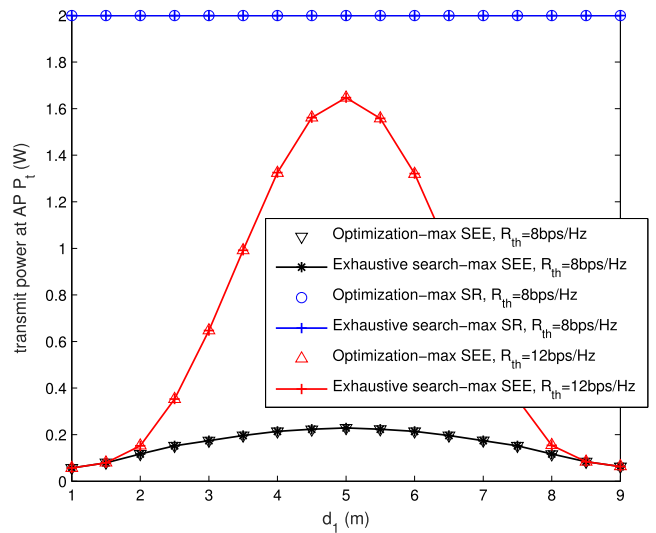


FIGURE 6. AP transmit power for different optimization problems with the implementation of STS strategy.

$d_1 \leq D/2$ , prolonging the duration  $\tau T$  of EH increases the transmit power at UR, further provides enough RF energy for information processing at UE. When UR moves towards UE with  $d_1 \geq D/2$ , smaller transmit power at AP and shortened EH duration not only contribute to less energy consumption but also larger SR thanks to longer duration of information transmission, finally resulting in higher SEE. For SR maximization problem, the maximum AP power and longer duration of information transmission enable the maximization of SR.

In Fig. 7, we plot SEE for both relaying strategies against  $d_1$ . The curves provide principles for relay placement to optimize SEE. As for the secure communication via one-way untrusted relay or two-way trusted relay [16], [26], the optimal secrecy performance is achieved with relay close to the destination. Unlike these scenarios, the untrusted relay

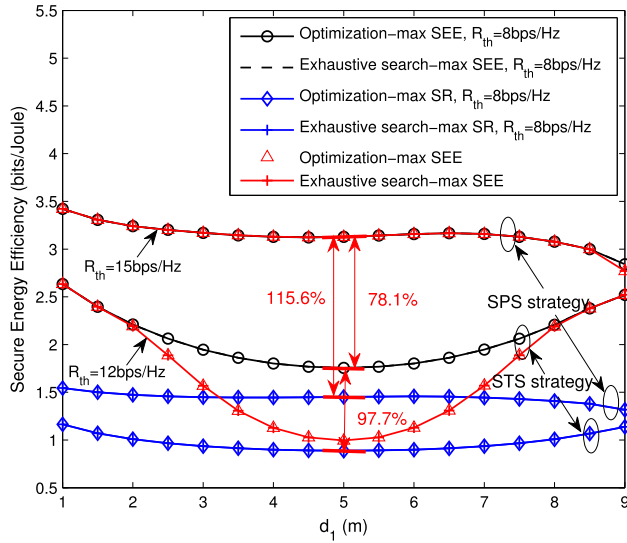


FIGURE 7. Comparison of SEE between different relaying strategies and optimization problems with varying  $d_1$ .

is suggested to be placed close to source under SPS strategy, and close to either source or destination under STS strategy. As discussed previously, SEE is dominated by path loss under SPS strategy, while by both path loss and information transmission duration under STS strategy. When UR moves towards AP, the improvement of SEE can be attributed to the weakened effect of path loss on  $\Xi_a$  and higher received jamming signal strength at UR. When UR moves towards UE, SPS-based relay makes secure performance worse since that the reduction of harvested energy at UR results in weak radiation power at UR and low SINR at AP. As for STS-based relay, reduced transmit power at UE jointly with extended information transmission duration improves the SINR and SEE at AP.

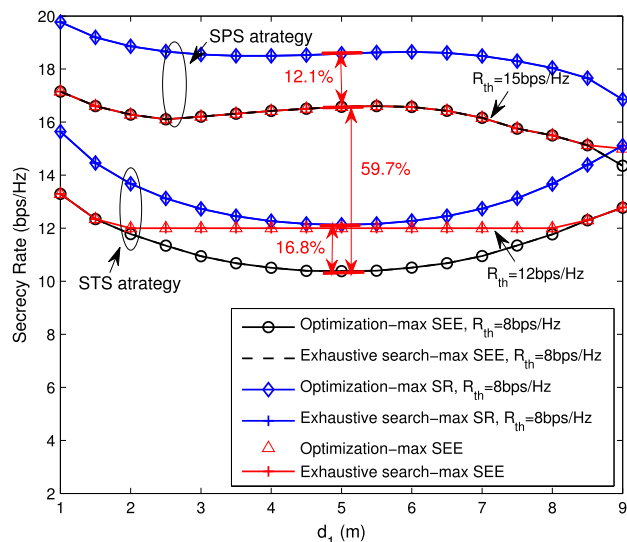


FIGURE 8. Comparison of SR between different relaying strategies and optimization problems with varying  $d_1$ .

In Fig. 8, we plot SR for both relaying strategies against  $d_1$ . It is revealed that the secure performance of SPS strategy

outperforms that of STS strategy over all  $d_1$  (approximate 59.7% gain on SR and 78.1% gain on SEE when SEE is maximized with  $d_1 = 5$ m). With a given relaying strategy, there exists a trade-off between the SR and SEE. For instance, 115.6% gain on SEE is at the expense of 12.1% loss in SR under SPS strategy, and 97.7% gain on SEE is at the expense of 16.8% loss in SR under STS strategy. The SPS strategy is preferable to system implementation due to its superiority in enhancing SEE while sacrificing only a small degree of SR.

### C. EFFECT OF SR TARGET

In Figs. 3 and 4, with the maximization of SEE under SPS strategy, when the achievable SR (larger than 15 bps/Hz according to the results in Fig. 8) is above target SR, the near-optimal solution remains unchanged in spite of the variation of SR target. In Figs. 5 and 6, to satisfy higher SR target under STS strategy, the enlarged  $P_t$  and the extended duration of information transmission bring huge benefits. When exorbitant SR is required, the relay system runs into outage state with SPS-based UR near UE and STS-based UR near the midpoint of AP-UE link.

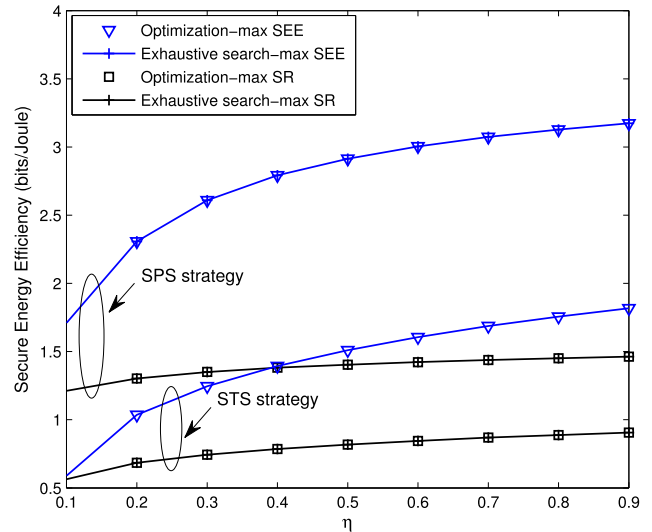


FIGURE 9. Comparison of SEE between different relaying strategies and optimization problems with varying EH conversion efficiency.

### D. EFFECT OF EH CONVERSION EFFICIENCY

In Fig. 9, we plot SEE against EH conversion efficiency  $\eta$  with  $R_{th} = 8$ bps/Hz. We notice that the SEE of SPS strategy outperforms that of STS strategy over all  $\eta$ . When larger fraction of energy can be extracted from RF signals, for both relay strategies, the gain on SEE becomes more obvious comparing with the SR maximization circumstances.

### E. CONVERGENCE OF THE PROPOSED ALGORITHM

In Fig. 10, the convergence of the proposed SRA algorithm is investigated when SPS strategy is applied at UR. With the increasing of iterations, the gap between the proposed algorithm and exhaustive search narrows down quickly. Finally, the proposed algorithm can achieve near-optimal

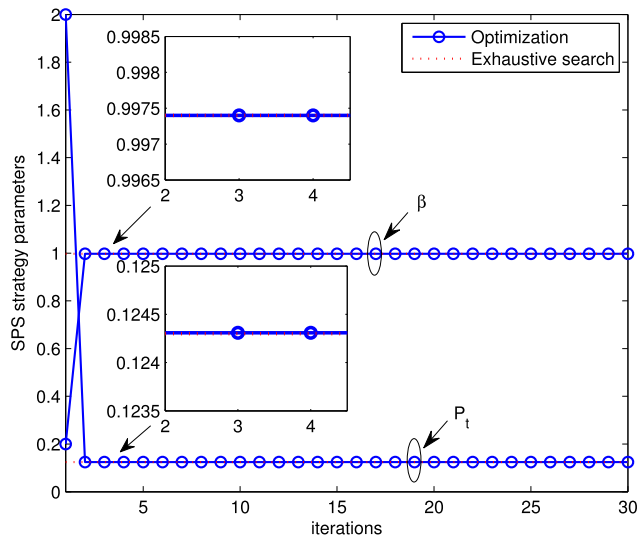


FIGURE 10. Convergence of the proposed algorithm for SEE optimization under SPS strategy with  $d_1 = 5m$ .

result, which confirms the effectiveness and convergence of the proposed algorithm.

## VI. CONCLUSION

In this paper, we have investigated the secure transmission in two-way untrusted SWIPT relaying system. Two secure SWIPT relaying strategies, namely SPS and STS, have been performed with AP-assisted jamming to improve security. SR and SEE maximization problems are formulated and solved for both strategies. Numerical results reveal that the SPS-based relay outperforms the STS-based relay with approximate 59.7% gain on SR and 78.1% gain on SEE. The optimal location of the untrusted relay is close to source under SPS strategy and close to either two ends of source-destination link under STS strategy, which is distinct from the conclusion in two-way trusted relay scenario. In future work, to better promote secure transmission in mobile scenario, appropriate mobile EH model and relay selection will be conducted.

## REFERENCES

- [1] S. Bi, Y. Zeng, and R. Zhang, "Wireless powered communication networks: An overview," *IEEE Wireless Commun.*, vol. 23, no. 2, pp. 10–18, Apr. 2016.
- [2] S. Bi, C. K. Ho, and R. Zhang, "Wireless powered communication: Opportunities and challenges," *IEEE Commun. Mag.*, vol. 53, no. 4, pp. 117–125, Apr. 2015.
- [3] X. Lu, P. Wang, D. Niyato, D. I. Kim, and Z. Han, "Wireless networks with RF energy harvesting: A contemporary survey," *IEEE Commun. Surveys Tuts.*, vol. 17, no. 2, pp. 757–789, 2nd Quart., 2015.
- [4] M. Xia and S. Aissa, "On the efficiency of far-field wireless power transfer," *IEEE Trans. Signal Process.*, vol. 63, no. 11, pp. 2835–2847, Jun. 2015.
- [5] L. Liu, R. Zhang, and K.-C. Chua, "Wireless information transfer with opportunistic energy harvesting," *IEEE Trans. Wireless Commun.*, vol. 12, no. 1, pp. 288–300, Jan. 2013.
- [6] A. A. Nasir, X. Zhou, S. Durrani, and R. A. Kennedy, "Relaying protocols for wireless energy harvesting and information processing," *IEEE Trans. Wireless Commun.*, vol. 12, no. 7, pp. 3622–3636, Jul. 2013.
- [7] X. Chen, D. W. K. Ng, and H.-H. Chen, "Secrecy wireless information and power transfer: Challenges and opportunities," *IEEE Wireless Commun.*, vol. 23, no. 2, pp. 54–61, Apr. 2016.

- [8] M. Liu and Y. Liu, "Power allocation for secure SWIPT systems with wireless-powered cooperative jamming," *IEEE Commun. Lett.*, vol. 21, no. 6, pp. 1353–1356, Jun. 2017.
- [9] H. Xing, K.-K. Wong, Z. Chu, and A. Nallanathan, "To harvest and jam: A paradigm of self-sustaining friendly jammers for secure AF relaying," *IEEE Trans. Signal Process.*, vol. 63, no. 24, pp. 6616–6631, Dec. 2015.
- [10] Y. Feng, Z. Yang, W.-P. Zhu, Q. Li, and B. Lv, "Robust cooperative secure beamforming for simultaneous wireless information and power transfer in amplify-and-forward relay networks," *IEEE Trans. Veh. Technol.*, vol. 66, no. 3, pp. 2354–2366, Mar. 2017.
- [11] Q. Li, Q. Zhang, and J. Qin, "Secure relay beamforming for SWIPT in amplify-and-forward two-way relay networks," *IEEE Trans. Veh. Technol.*, vol. 65, no. 11, pp. 9006–9019, Nov. 2016.
- [12] N.-P. Nguyen, T. Q. Duong, H. Q. Ngo, Z. Hadzi-Velkov, and L. Shu, "Secure 5G wireless communications: A joint relay selection and wireless power transfer approach," *IEEE Access*, vol. 4, pp. 3349–3359, 2016.
- [13] L. Jiang, C. Qin, X. Zhang, and H. Tian, "Secure beamforming design for SWIPT in cooperative D2D communications," *China Commun.*, vol. 14, no. 1, pp. 20–33, Jan. 2017.
- [14] F. Zhou, Z. Li, J. Cheng, Q. Li, and J. Si, "Robust AN-aided beamforming and power splitting design for secure MISO cognitive radio with SWIPT," *IEEE Trans. Wireless Commun.*, vol. 16, no. 4, pp. 2450–2464, Apr. 2017.
- [15] M. Zhao, X. Wang, and S. Feng, "Joint power splitting and secure beamforming design in the multiple non-regenerative wireless-powered relay networks," *IEEE Commun. Lett.*, vol. 19, no. 9, pp. 1540–1544, Sep. 2015.
- [16] S. S. Kalamkar and A. Banerjee, "Secure communication via a wireless energy harvesting untrusted relay," *IEEE Trans. Veh. Technol.*, vol. 66, no. 3, pp. 2199–2213, Mar. 2017.
- [17] A. Mabrouk, A. El Shafie, K. Tourki, and N. Al-Dhahir, "Adaptive secure transmission for RF-EH untrusted relaying with alien eavesdropping," *IEEE Commun. Lett.*, vol. 21, no. 11, pp. 2516–2519, Nov. 2017.
- [18] D. Wang, B. Bai, W. Chen, and Z. Han, "Secure green communication via untrusted two-way relaying: A physical layer approach," *IEEE Trans. Commun.*, vol. 64, no. 5, pp. 1861–1874, May 2016.
- [19] D. Wang, B. Bai, W. Chen, and Z. Han, "Achieving high energy efficiency and physical-layer security in AF relaying," *IEEE Trans. Wireless Commun.*, vol. 15, no. 1, pp. 740–752, Jan. 2016.
- [20] J. Mo, M. Tao, Y. Liu, and R. Wang, "Secure beamforming for MIMO two-way communications with an untrusted relay," *IEEE Trans. Signal Process.*, vol. 62, no. 9, pp. 2185–2199, May 2014.
- [21] H.-M. Wang, Q. Yin, and X.-G. Xia, "Distributed beamforming for physical-layer security of two-way relay networks," *IEEE Trans. Signal Process.*, vol. 60, no. 7, pp. 3532–3545, Jul. 2012.
- [22] H.-M. Wang, M. Luo, Q. Yin, and X.-G. Xia, "Hybrid cooperative beamforming and jamming for physical-layer security of two-way relay networks," *IEEE Trans. Inf. Forensics Security*, vol. 8, no. 12, pp. 2007–2020, Dec. 2013.
- [23] H. Xu, L. Sun, P. Ren, Q. Du, and Y. Wang, "Cooperative privacy preserving scheme for downlink transmission in multiuser relay networks," *IEEE Trans. Inf. Forensics Security*, vol. 12, no. 4, pp. 825–839, Apr. 2017.
- [24] H. Wu, X. Tao, Z. Han, N. Li, and J. Xu, "Secure transmission in MISOME wiretap channel with multiple assisting jammers: Maximum secrecy rate and optimal power allocation," *IEEE Trans. Commun.*, vol. 65, no. 2, pp. 775–789, Feb. 2017.
- [25] W. Dinkelbach, "On nonlinear fractional programming," *Manage. Sci.*, vol. 13, no. 7, pp. 492–498, 1967.
- [26] Y. Zeng, H. Chen, and R. Zhang, "Bidirectional wireless information and power transfer with a helping relay," *IEEE Commun. Lett.*, vol. 20, no. 5, pp. 862–865, May 2016.
- [27] H. Wu, X. Tao, N. Zhang, D. Wang, S. Zhang, and X. Shen, "On base station coordination in cache-and energy harvesting-enabled hetnets: A stochastic geometry study," *IEEE Trans. Commun.*, to be published.
- [28] Z. Qin, X. Gan, J. Wang, L. Fu, and X. Wang, "Capacity of social-aware wireless networks with directional antennas," *IEEE Trans. Commun.*, vol. 65, no. 11, pp. 4831–4844, Nov. 2017.
- [29] H.-N. Dai, K.-W. Ng, M. Li, and M.-Y. Wu, "An overview of using directional antennas in wireless networks," *Int. J. Commun. Syst.*, vol. 26, no. 4, pp. 413–448, 2013.
- [30] J. Peng, P. Hong, and K. Xue, "Energy-aware cellular deployment strategy under coverage performance constraints," *IEEE Trans. Wireless Commun.*, vol. 14, no. 1, pp. 69–80, Jan. 2015.
- [31] Z. Ding et al., "Application of smart antenna technologies in simultaneous wireless information and power transfer," *IEEE Commun. Mag.*, vol. 53, no. 4, pp. 86–93, Apr. 2015.

- [32] B. Gurakan, O. Ozel, J. Yang, and S. Ulukus, "Energy cooperation in energy harvesting communications," *IEEE Trans. Commun.*, vol. 61, no. 12, pp. 4884–4898, Dec. 2013.
- [33] S. Boyd and L. Vandenberghe, *Convex Optimization*. Cambridge, U.K.: Cambridge Univ. Press, 2004.



**JIAZHEN ZHANG** received the B.E. degree in communication engineering from the Beijing University of Posts and Telecommunications, Beijing, China, in 2015, where she is currently pursuing the Ph.D. degree in information and communication engineering. Her research interests include the area of wireless communications, with current emphasis on physical-layer security and non-orthogonal multiple access.



**XIAOFENG TAO** (SM'13) received the B.S. degree in electrical engineering from Xi'an Jiaotong University, Xi'an, China, in 1993, and the M.S.E.E. and Ph.D. degrees in telecommunication engineering from the Beijing University of Posts and Telecommunications (BUPT), Beijing, China, in 1999 and 2002, respectively.

He was a Visiting Professor with Stanford University, Stanford, CA, USA, from 2010 to 2011, and the Chief Architect with the Chinese National FuTURE Fourth-Generation (4G) TDD working group from 2003 to 2006. He established the 4G TDD CoMP trial network in 2006. He is currently a Professor with BUPT. He has authored or co-authored over 120 papers in 4G and beyond 4G and an inventor or co-inventor of 50 patents. He is a fellow of the Institution of Engineering and Technology.



**HUICI WU** received the B.S. degree from the Information Engineering School, Communication University of China, Beijing, China, in 2013. She is currently pursuing the Ph.D. degree in communications and information systems with the Beijing University of Posts and Telecommunications, Beijing. From 2016 to 2017, she was a Visiting Student with the Broadband Communications Research Group, Department of Electrical and Computer Engineering, University of Waterloo, Waterloo, ON, Canada. Her research interests include the area of wireless communications and networks, with current emphasis on cooperation and physical-layer security in heterogeneous networks.



**XUEFEI ZHANG** received the B.S. and Ph.D. degrees in telecommunications engineering from the Beijing University of Posts and Telecommunications (BUPT) in 2010 and 2015, respectively. She is currently with the National Engineering Laboratory, BUPT. Her research area includes multi-access edge computing, machine technology communications, intelligent transportation system, stochastic geometry, and dynamic programming.

...